

Porous Polycaprolactone Scaffold Engineered with Naringin Loaded Bovine Serum Albumin Nanoparticles for Bone Tissue Engineering

Balraj Sundaram and M. C. John Milton*

P.G. and Research Department of Advanced Zoology and Biotechnology,
Loyola College, Chennai, Tamil Nadu, India.

<http://dx.doi.org/10.13005/bbra/2580>

(Received: 03 November 2017; accepted: 07 November 2017)

A biodegradable three-dimensional scaffolds have gathered attention and are widely studied for bone tissue engineering applications. In the present study, porous polycaprolactone scaffold entrapped with naringin loaded bovine serum albumin nanoparticles (PS-N-BSANP) has been engineered. Further, the prepared nanoparticles and interconnected porous scaffolds were characterized by scanning electron microscopy, X-ray diffraction and fourier transform infrared spectroscopy analysis. X-ray diffraction showed amorphization of naringin in PS-N-BSANP. In addition, sustained naringin release profile was observed from PS-N-BSANP for 12 days which showed a cumulative release of 52.54 micromolar (μM). Furthermore, conditioned medium from PS-N-BSANP showed an increased calcium deposition and collagen matrix formation under osteogenic conditions with C3H10T1/2 cell line. These results suggest that PS-N-BSANP enhanced the osteogenic differentiation potential in bone tissue engineering applications due to the controlled release of naringin.

Keywords: Naringin, Polycaprolactone Porous Scaffold, Bovine Serum Albumin Nanoparticles, Bone Tissue Engineering, C3H10T1/2 cell line.

In recent years, three-dimensional biodegradable scaffolds has gathered more attention in various tissue engineering fields for reconstruction of damaged tissues¹. In general, cells require an three-dimensional matrix for cell adhesion, proliferation and controlled environment for tissue restoration². Hence, three-dimensional scaffolds are widely used as an extracellular matrix in tissue repair applications³. Moreover, three-dimensional scaffolds have been synthesized from many different types of aliphatic polyesters and natural polymers for therapeutic applications due

to its excellent properties such as biodegradability, biocompatibility and mechanical strength⁴. Among those polymers, polycaprolactone is Food and Drug Administration approved biodegradable material to construct the porous scaffolds for long-term implants^{4,5}.

Regeneration of bone fracture with a bone loss of 3cm is tedious process⁶. Therefore, biodegradable porous scaffolds are extensively evaluated as an alternative for autologous and allogeneic approaches in bone tissue repair⁶. In addition, controlled release of bioactive molecules

*Corresponding author E-mail: biotechres17@gmail.com

This is an Open Access article licensed under a Creative Commons Attribution-NonCommercial-ShareAlike 4.0 International License (<https://creativecommons.org/licenses/by-nc-sa/4.0/>), which permits unrestricted Non Commercial use, distribution and reproduction in any medium, provided the original work is properly cited.

Published by Oriental Scientific Publishing Company © 2017



from the porous scaffolds could increase the therapeutic potential in bone regeneration⁶. Naringin is a flavanone glycoside that has shown enormous potential such as antiinflammatory, antioxidant, anticancer, antidiabetic *etc*⁷. Also, naringin enhances the proliferation and osteogenic differentiation of human bone marrow-derived mesenchymal stem cells⁸.

We propose controlled release of naringin from a three-dimensional porous scaffold could increase its therapeutic potential in bone regeneration. In this study, three-dimensional porous polycaprolactone scaffold carrying bovine serum albumin nanoparticles loaded with naringin is fabricated and evaluated for its *in vitro* osteogenic potential using C3H10T1/2 cell line.

MATERIALS AND METHODS

Polycaprolactone (average Mn 80,000), Naringin ($\geq 95\%$ (HPLC)), β -glycerophosphate, Dexamethasone, Ascorbic acid, Direct red 80, Hematoxylin were purchased from Sigma-Aldrich (St. Louis, MO). Bovine serum albumin (BSA) fraction V (pH 6-7) purchased from Sisco Research Laboratories Pvt. Ltd., Mumbai, India. Dulbecco's modified eagle medium-low glucose (DMEM-LG), Antibiotic-antimycotic solution, Dulbecco's phosphate buffered saline (DPBS), Trypsin-ethylenediaminetetraacetic acid (Trypsin-EDTA) solution, 3-(4,5-Dimethyl-2-thiazolyl)-2,5-diphenyltetrazolium bromide (MTT), Picric acid, Silver nitrate were purchased from Himedia, Mumbai, India. Fetal bovine serum (FBS) was purchased from PAN Biotech, Germany. All other chemicals and solvents used were of analytical grade.

Preparation of naringin loaded bovine serum albumin nanoparticles (N-BSANP)

N-BSANP was synthesized by coacervation process as described earlier^{6,9}. In brief, naringin (2% w/w) was added to the 2% (w/v) of BSA in deionized water followed by one hour incubation at room temperature. After incubation, ethanol was added dropwise until turbidity under constant stirring. Further, coacervates were hardened with 8% glutaraldehyde, incubated for 2 hours under constant stirring. After incubation, nanoparticles were obtained by centrifugation at 18000g, 4°C for 30 minutes. The pellet was

suspended in DPBS and washed thrice and freeze-dried. The entrapment efficiency was calculated from the amount of free naringin present in the supernatant using the formula

$$\text{Entrapment Efficiency} = [(T_{\text{Nar}} - F_{\text{Nar}})/T_{\text{Nar}}] \times 100\%$$

Where, T_{Nar} is the total amount of naringin added and F_{Nar} is the free naringin in the supernatant.

Preparation of porous polycaprolactone scaffold entrapped with naringin loaded bovine serum albumin nanoparticles (PS-N-BSANP)

PS-N-BSANP was engineered by solvent casting and particulate leaching method^{6,10}. Polycaprolactone (10% w/v) was dissolved in equal volumes of dichloromethane and ethanol. N-BSANP (5% w/w) was added to the polycaprolactone solution and sonicated on ice to achieve the homogeneous mixture. To this, finely ground sucrose (1:5 ratio; polycaprolactone to sucrose) was added and stirred to make a uniform slurry, cast into glass molds and dried at room temperature. Further, sucrose was leached out with deionized water to form a porous structure followed by treatment with 0.5M NaOH for 4 hours to impart hydrophilicity. The scaffolds were neutralized by repeated washing with deionized water and 50% ethanol. Furthermore, scaffolds were stabilized using an absolute ethanol and washed with DPBS, UV sterilized for 30 minutes. Polycaprolactone scaffold prepared the same without N-BSANP was treated as control (PS).

Characterization of prepared nanoparticles and porous scaffolds

Scanning electron microscopy (SEM)

To determine the size of the prepared nanoparticles, N-BSANP was sputtered with gold and analyzed by SEM (TESCAN VEGA3 SBU) with 25kV applied voltage and 25000x magnifications. The average size of the nanoparticles were calculated manually by measuring 30 particles, selected randomly from SEM image using ImageJ software (ImageJ 1.51j8, National Institutes of Health, USA) and the results were expressed as mean \pm standard deviation. Similarly, the fabricated scaffolds were cut into small pieces and sputtered with gold, morphology of the scaffolds were observed by SEM with an applied voltage of 10kV and 200 μ M magnifications.

X-ray diffraction (XRD)

The prepared nanoparticles and porous

scaffolds were characterized by X-ray diffraction using the PANalytical X'Pert PRO (Almelo, The Netherlands) with a current of 30mA and a load of 40kV tension. The 2θ scan ranges from 10° – 100° with a step size of 0.0167.

Fourier transform infrared spectroscopy (FTIR)

Samples (3mg) were mixed with 300 mg of potassium bromide and the pellet was made with mechanical pellet maker. Further, the samples were analyzed in the range of 4000 – 500cm^{-1} with a resolution of 1cm^{-1} using an Alpha FTIR spectrophotometer (Bruker Optics, Mumbai, India).

Naringin release from PS-N-BSANP

PS-N-BSANP was cut into $1\text{cm} \times 1\text{cm}$ and incubated in 2ml of DPBS under static condition. At fixed time intervals, $700\mu\text{l}$ was removed and replaced with equal amounts of DPBS, read at 284 nm using UV-Vis spectrophotometer (Systronics, India)¹¹. The concentration of released naringin was obtained from the naringin standard curve.

Cell culture

C3H10T1/2 (Mouse mesenchymal cell line) was purchased from National Centre for Cell Sciences (NCCS, Pune, India) and cultured in undifferentiated state using complete culture medium (DMEM-LG supplemented with 10% FBS and 1% antibiotic-antimycotic solution) under standard culture conditions (37°C , 5% CO_2 humidified incubator). The cells were trypsinized and subcultured using trypsin-EDTA solution at 80% confluence.

Preparation of conditioned media (CM)

The sterile scaffolds (PS and PS-N-BSANP) were incubated in 1ml of complete culture medium under standard culture conditions. Then, the media were collected and replaced with fresh complete culture medium every day. The collected media were termed as conditioned media. Furthermore, CM obtained from PS scaffold termed as CM-PS, from PS-N-BSANP scaffold as CM-PS-N-BSANP and used for further studies.

Evaluation of *in vitro* osteogenic potential

Cells (5×10^4) were seeded in 12 well culture plates and allowed to attach overnight under complete culture medium. The groups were labeled as CM-PS (control) and CM-PS-N-BSANP. Further, the complete culture medium was replaced in respective groups with CM and osteogenic medium (DMEM-LG containing 10%

FBS, 1% antibiotic-antimycotic solution, $100\mu\text{g/ml}$ ascorbic acid, 20nM dexamethasone and 20mM β -glycerophosphate) in equal volumes with a change of media every day. To determine the cytotoxicity and osteogenic potential of CM the following assays were performed.

MTT assay

The cytotoxicity of the CM was evaluated by MTT assay^{3,6}. On day 3, the cells were rinsed with sterile DPBS followed by MTT solution (0.5mg/ml in DPBS) was added and then incubated for four hours to form formazan crystals. After incubation, the formazan crystals were solubilized with an appropriate volume of DMSO and read at 590nm using UV-Vis spectrophotometer.

von Kossa and picrosirius red staining

von Kossa staining¹² and picrosirius red staining¹³ were done to visualize the calcium deposition and collagen matrix formation respectively. On day 12, wells were washed with DPBS and fixed with 10% neutral buffered formalin.

For von Kossa staining, silver nitrate solution (1%) was added and exposed to ultraviolet light for 45 minutes. Further, to stop the reaction 5% sodium thiosulfate solution was added followed by washing with distilled water. Calcium deposits stained as black coloured crystals were observed under microscope at 10x magnification.

For picrosirius red staining, cells were incubated with Weigert's hematoxylin for 8 minutes and washed with distilled water. Further, picrosirius red was added and incubated for one hour and washed with acidified water to remove the excess stain. Furthermore, red coloured stained collagen matrix formation was observed at 10x magnification under microscope.

Statistical analysis

The results of MTT assay were expressed as mean \pm standard deviation. The statistical analysis was evaluated by unpaired student's t-test using GraphPad PRISM 5.01 (San Diego, CA) and the significant difference ($p < 0.05$) was considered as statistically significant.

RESULTS AND DISCUSSION

Characterization of the nanoparticles and porous scaffolds

The nanoparticles were synthesized by

coacervation process and the average size of prepared nanoparticles were found as 203.21 ± 38.99 nm for N-BSANP (Fig. 1A). These particles did not form agglomerates and were spherical in shape. BSA is a biodegradable protein which is extensively used to synthesize the nanoparticles for sustained release of bioactive molecules in various drug delivery applications due to its excellent properties such as biocompatible, nontoxic, nonimmunogenic *etc*^{14,15}.

Further, the SEM images of PS (Fig. 1B) and PS-N-BSANP (Fig. 1C) showed interconnected porous structure, which is a most important aspect for cell penetration into the scaffolds. The scaffolds with highly interconnected porous network are considered advantageous for cell migration, attachment, tissue ingrowth, angiogenesis and also it could supports to transport nutrients and wastes¹⁶.

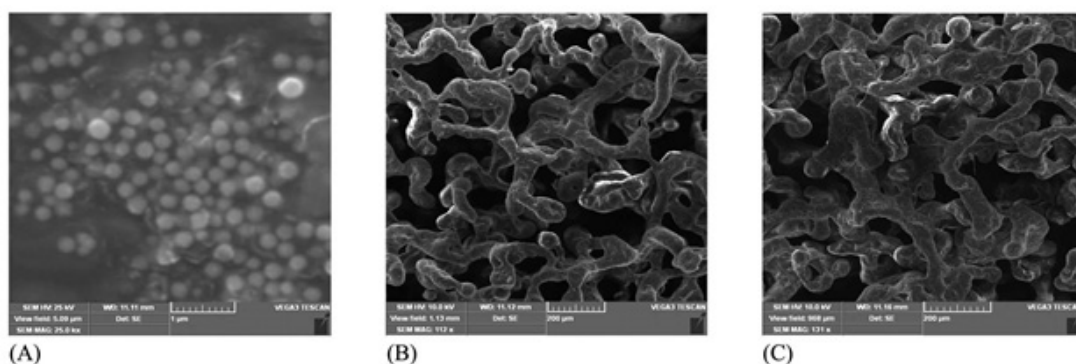


Fig. 1. SEM images of nanoparticles and porous scaffolds. Where, (A) - Naringin loaded bovine serum albumin nanoparticles; (B) - Polycaprolactone scaffold; (C) - Polycaprolactone scaffold entrapped with naringin loaded bovine serum albumin nanoparticles

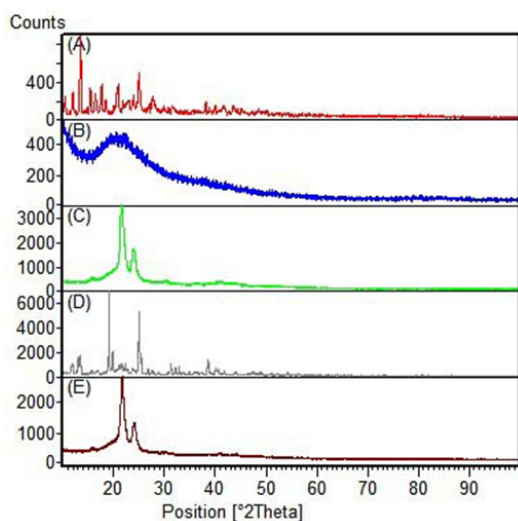


Fig. 2. X-ray diffraction spectra. Where, (A) - Naringin; (B) - Naringin loaded bovine serum albumin nanoparticles; (C) - Polycaprolactone scaffold; (D) - Polycaprolactone scaffold entrapped with naringin loaded bovine serum albumin nanoparticles - unleached (before sucrose leaching out); (E) - Polycaprolactone scaffold entrapped with naringin loaded bovine serum albumin nanoparticles (after leaching out)

XRD analysis was done to determine the crystallinity of prepared nanoparticles and porous scaffolds, the results are shown in Fig. 2. Naringin diffraction spectra (Fig. 2A) showed many numbers of intense peaks¹⁷. Further, the broad diffraction peak was seen in N-BSANP spectra (Fig. 2B) corresponds to amorphous BSA, also absence of naringin peaks implies amorphization of naringin during encapsulation which increases the dissolution of hydrophobic drugs¹⁸. Also, two semicrystalline peaks were observed for PS (at 2θ of 21.6° and 24°) (Fig. 2C) and PS-N-BSANP (at 2θ of 21.8° and 24.1°) (Fig. 2E) which corresponds to polycaprolactone⁶. In addition, PS-N-BSANP unleached spectra (Fig. 2D) showed many intense peaks corresponding to sucrose compared to PS-N-BSANP scaffold, which confirmed that the sucrose has leached out completely in PS-N-BSANP scaffold.

FTIR spectra revealed the characteristic peaks for prepared nanoparticles and porous scaffolds. Naringin spectra (Fig. 3A) showed the characteristic peaks at 1647.7 cm^{-1} , 1519.1 cm^{-1} , 1456.8 cm^{-1} , 1363.4 cm^{-1} , 1264.1 cm^{-1} , 1178.6 cm^{-1} ,

1137.2 cm^{-1} , 1088.8 cm^{-1} , 888.1 cm^{-1} , 835.7 cm^{-1} and 639 cm^{-1} ¹⁹. Further, N-BSANP characteristic peaks were showed in Fig. 3B. In N-BSANP, the bands at 1647.6 cm^{-1} , 1270.2 cm^{-1} and 1173.9 cm^{-1} indicates the presence of naringin in prepared nanoparticles which confirms that naringin was not modified chemically during entrapment process. As previously reported, a strong band at 1735.33 cm^{-1} (C=O stretching) and 2863.21 cm^{-1} (asymmetric CH_2 -stretching) were observed for PS scaffold (Fig. 3C) which corresponds to aliphatic polyester of polycaprolactone²⁰. Similarly, characteristic peaks of polycaprolactone were observed at 1731.62 cm^{-1} , 2944.69 cm^{-1} (symmetric CH_2 -stretching) and 2865.55 cm^{-1} in PS-N-BSANP scaffold (Fig. 3D). Also, the band for bovine serum albumin nanoparticles was observed at 1243.05 cm^{-1} ²¹ and also the bands at 1469.31 cm^{-1} and 1367.80 cm^{-1} confirmed the naringin characteristic peaks in PS-N-BSANP scaffold. These results indicates that there was no chemical modification of naringin nor chemical bonding to bovine serum albumin

nanoparticles and polycaprolactone during PS-N-BSANP scaffold fabrication.

Naringin release from PS-N-BSANP

The nanoparticles were synthesized by coacervation process and the entrapment efficiency of naringin was found to be 97.38%. Sustained release of naringin was analyzed from porous PS-N-BSANP scaffold and the cumulative release was found to be 52.54 micromolar (μM) at the end of 12 days (Fig. 4). In general, drug delivery systems helps to deliver bioactive agents in a controlled manner at the targeted site²². Incorporation of various drug delivery systems into three-dimensional scaffolds have been gathered more consideration for delivery of bioactive molecules with desired concentrations which can be more advantageous in bone tissue engineering approach^{22,23}. Previous studies have reported that, various drugs, growth factors, antiinflammatories and antibiotics have successfully incorporated into the three-dimensional scaffolds and have demonstrated clinical potentials in the treatment

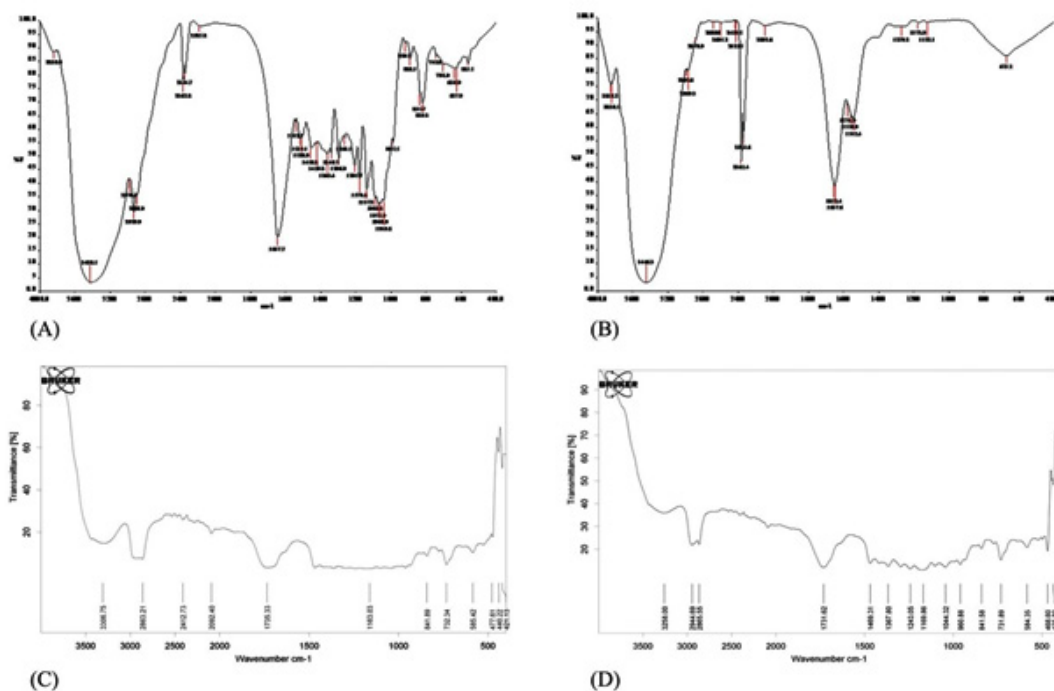


Fig. 3. Fourier transform infrared spectroscopy analysis of nanoparticles and porous scaffolds. Where, (A) - Naringin; (B) - Naringin loaded bovine serum albumin nanoparticles; (C) - Polycaprolactone scaffold; (D) - Polycaprolactone scaffold entrapped with naringin loaded bovine serum albumin nanoparticles

and management of bone-related pathologies^{22,24,25}. Further, targeted drug delivery improves the drug absorption and intracellular diffusion, sustained release for longer time, enhances drug efficacy and also it could reduce the drug degradation²⁶. The naringin release profile suggests that N-BSANP was successfully entrapped into the porous polycaprolactone scaffold and it releases naringin in a controlled manner.

In vitro osteogenic potential of CM

The MTT assay showed that the conditioned media from the fabricated porous scaffolds were not toxic with C3H10T1/2 cell line (Fig. 5). The absorbance values of CM-PS-N-BSANP group showed significant increase ($P < 0.05$) in cell population compared with control. Previously reported studies has shown proliferative effect of naringin on human bone mesenchymal

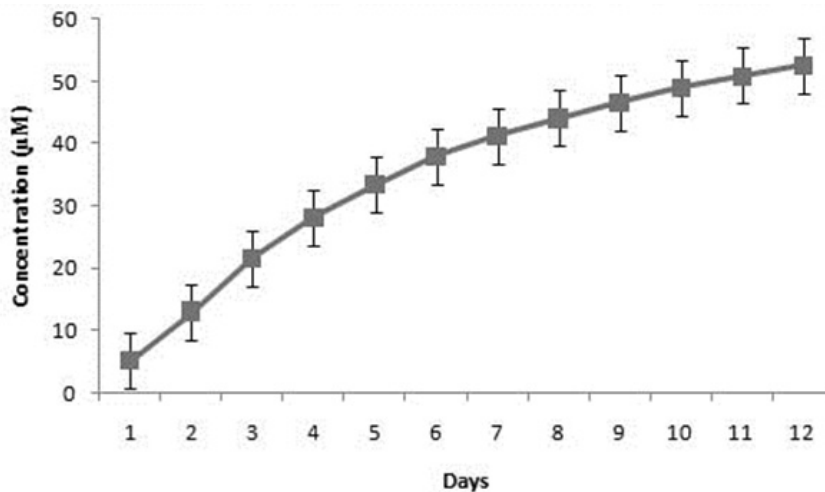


Fig. 4. Cumulative naringin release from naringin loaded bovine serum albumin nanoparticles entrapped polycaprolactone scaffold

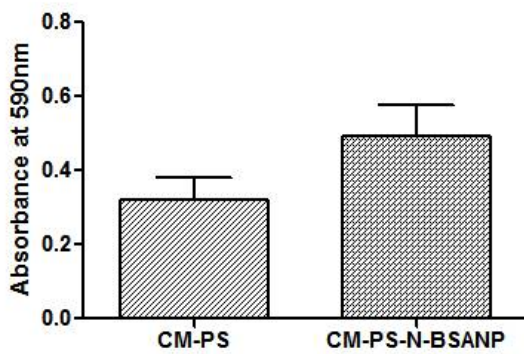


Fig. 5. MTT assay. Where, CM-PS - Conditioned medium obtained from polycaprolactone scaffold; CM-PS-N-BSANP - Conditioned medium obtained from naringin loaded bovine serum albumin nanoparticles entrapped polycaprolactone scaffold

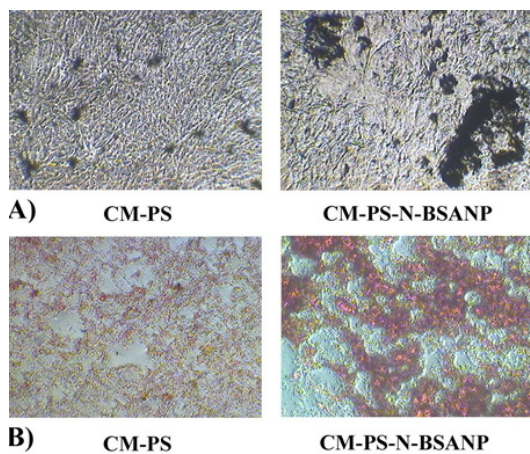


Fig. 6. (A) von Kossa staining for calcium deposition; (B) Picrosirius red staining for collagen matrix formation. Where, CM-PS - Conditioned medium obtained from polycaprolactone scaffold; CM-PS-N-BSANP - Conditioned medium obtained from naringin loaded bovine serum albumin nanoparticles entrapped polycaprolactone scaffold

stem cells⁸, MC3T3-E1, MG63²⁷, human adipose derived mesenchymal stem cells²⁸, rat osteoblast-like UMR-106 cells^{29,30} etc in a dose-dependent manner. Further, adipose-derived mesenchymal stem cell seeded polycaprolactone scaffold showed a good proliferative effect of cells on day 14 with osteogenic differentiation medium³¹. This MTT results inferred that the conditioned medium from porous polycaprolactone scaffolds enhanced the cell proliferation.

Osteogenic differentiation of CM-PS-N-BSANP was evaluated using C3H10T1/2 cell line by von Kossa and picosirius red staining. Increased calcium deposition (Fig. 6A) and collagen matrix formation (Fig. 6B) were observed in CM-PS-N-BSANP by von Kossa and picosirius red staining respectively compared with control. A previous study reported that, increased mineralization was observed with bone marrow stromal cells in a dose-dependent naringin concentrations³². Further, sustained release of naringin showed an increased calcium deposition with the MC3T3-E1 osteoblasts³³. These results implies that the porous polycaprolactone scaffold entrapped with naringin loaded bovine serum albumin nanoparticles showed the sustained release of naringin and it enhanced the calcium deposition and collagen matrix formation under osteogenic conditions.

CONCLUSION

In this study, biodegradable PS-N-BSANP porous scaffold was engineered and characterized by SEM, XRD and FTIR analysis. Further, cumulative naringin release profile from PS-N-BSANP scaffold showed sustained release of naringin for 12 days. Furthermore, conditioned media from PS-N-BSANP scaffold was not toxic and it showed an increasing calcium deposition and collagen matrix formation which is highly desired in bone tissue engineering. Thus, we conclude that porous PS-N-BSANP scaffold can serve as an osteoconductive bone graft material in bone tissue engineering applications.

REFERENCES

1. Cui, Z., Nelson, B., Peng, Y., Li, K., Pilla, S., Li, W.-J., Turng, L.-S., Shen, C. Fabrication and characterization of injection molded poly (μ -caprolactone) and poly (μ -caprolactone)/hydroxyapatite scaffolds for tissue engineering. *Mater. Sci. Eng. C*, 2012; **32**: 1674–81.
2. Reignier, J., Huneault, M.A. Preparation of interconnected poly(μ -caprolactone) porous scaffolds by a combination of polymer and salt particulate leaching. *Polymer (Guildf)*, 2006; **47**: 4703–17.
3. Bhardwaj, N., Kundu, S.C. Silk fibroin protein and chitosan polyelectrolyte complex porous scaffolds for tissue engineering applications. *Carbohydr. Polym.*, 2011; **85**: 325–33.
4. Thadavirul, N., Pavasant, P., Supaphol, P. Development of polycaprolactone porous scaffolds by combining solvent casting, particulate leaching, and polymer leaching techniques for bone tissue engineering. *J. Biomed. Mater. Res. Part A*, 2014; **102**: 3379–92.
5. Jang, C.H., Kim, M.S., Cho, Y.B., Jang, Y.S., Kim, G.H. Mastoid obliteration using 3D PCL scaffold in combination with alginate and rhBMP-2. *Int. J. Biol. Macromol.*, 2013; **62**: 614–22.
6. Kamath, M.S., Ahmed, S.S.S.J., Dhanasekaran, M., Santosh, S.W. Polycaprolactone scaffold engineered for sustained release of resveratrol: therapeutic enhancement in bone tissue engineering. *Int. J. Nanomedicine*, 2014; **9**: 183–95.
7. Adil, M., Visnagri, A., Kumar, V.S., Kandhare, A.D., Ghosh, P., Bodhankar, S.L. Protective effect of naringin on sodium arsenite induced testicular toxicity via modulation of biochemical perturbations in experimental rats. *Pharmacologia*, 2014; **5**: e234.
8. Peng-Zhang, Dai, K., Yan, S., Yan, W., Chao-Zhang, Chen, D., Bo-Xu, Xu, Z. Effects of naringin on the proliferation and osteogenic differentiation of human bone mesenchymal stem cell. *Eur. J. Pharmacol.*, 2009; **607**: 1–5.
9. Merodio, M., Arnedo, A., Renedo, M.J., Irache, J.M. Ganciclovir-loaded albumin nanoparticles: characterization and *in vitro* release properties. *Eur. J. Pharm. Sci.*, 2001; **12**: 251–9.
10. Chuenjitkuntaworn, B., Inrung, W., Damrongsri, D., Mekaapiruk, K., Supaphol, P., Pavasant, P. Polycaprolactone/hydroxyapatite composite scaffolds: Preparation, characterization, and *in vitro* and *in vivo* biological responses of human primary bone cells. *J. Biomed. Mater. Res. Part A*, 2010; **94A**: 241–51.
11. Ranjith, R., Balraj, S., Ganesh, J., Milton, M.C.J. Effect of Flow Rate on Fiber Morphology and Naringin Release of Electrospun Naringin Loaded Polycaprolactone Nanofibers. *Int. J. Sci. Res. Sci. Technol.*, 2017; **3**(7): 05–08.
12. Dhanasekaran, M., Indumathi, S., Lissa, R.P.,

- Harikrishnan, R., Rajkumar, J.S., Sudarsanam, D. A comprehensive study on optimization of proliferation and differentiation potency of bone marrow derived mesenchymal stem cells under prolonged culture condition. *Cytotechnology*, 2013; **65**: 187–97.
13. Lilliu, M.A., Seo, Y.J., Isola, M., Charbonneau, A.M., Zeitouni, A., El-Hakim, M., Tran, S.D. Natural extracellular matrix scaffolds recycled from human salivary digests: a morphometric study. *Oral Dis.*, 2016; **22**: 313–23.
14. Yu, Z., Yu, M., Zhang, Z., Hong, G., Xiong, Q. Bovine serum albumin nanoparticles as controlled release carrier for local drug delivery to the inner ear. *Nanoscale Res. Lett.*, 2014; **9**: 343.
15. Lohcharoenkal, W., Wang, L., Chen, Y.C., Rojanasakul, Y. Protein nanoparticles as drug delivery carriers for cancer therapy. *Biomed Res. Int.*, 2014; 2014: 180549.
16. Koupaei, N., Karkhaneh, A. Porous crosslinked polycaprolactone hydroxyapatite networks for bone tissue engineering. *Tissue Eng. Regen. Med.*, 2016; **13**: 251–60.
17. Ranjith, R., Balraj, S., Ganesh, J., Milton, M.C.J. Electrospun Polycaprolactone Nanofibers for Sustained Release of Naringin. *Int. J. Sci. Res. Sci. Technol.*, 2017; **3**(6): 235–8.
18. Li, C., Zhang, D., Guo, H., Hao, L., Zheng, D., Liu, G., Shen, J., Tian, X., Zhang, Q. Preparation and characterization of galactosylated bovine serum albumin nanoparticles for liver-targeted delivery of oridonin. *Int. J. Pharm.*, 2013; **448**: 79–86.
19. Sahu, N., Soni, D., Chandrashekhar, B., Satpute, D.B., Saravanadevi, S., Sarangi, B.K., Pandey R.A. Synthesis of silver nanoparticles using flavonoids: hesperidin, naringin and diosmin, and their antibacterial effects and cytotoxicity. *Int. Nano Lett.*, 2016; **6**: 173–81.
20. Mendes, J.B.E., Riekes, M.K., de Oliveira, V.M., Michel, M.D., Stulzer, H.K., Khalil, N.M., Zawadzki, S.F., Mainardes, R.M., Farago, P.V. PHBV/PCL Microparticles for Controlled Release of Resveratrol: Physicochemical Characterization, Antioxidant Potential, and Effect on Hemolysis of Human Erythrocytes. *Sci. World J.*, 2012; 2012: 542937.
21. Rohiwal, S.S., Pawar, S.H. Synthesis and Characterization Of Bovine Serum Albumin Nanoparticles As A Drug Delivery Vehicle. *Int. J. Pharma Bio Sci.*, 2014; **5**: 51–7.
22. Mouriño, V., Boccaccini, A.R. Bone tissue engineering therapeutics: controlled drug delivery in three-dimensional scaffolds. *J. R. Soc. Interface.*, 2010; **7**: 209–27.
23. Baroli, B. From natural bone grafts to tissue engineering therapeutics: Brainstorming on pharmaceutical formulative requirements and challenges. *J. Pharm. Sci.*, 2009; **98**: 1317–75.
24. Fereshteh, Z., Fathi, M., Bagri, A., Boccaccini, A.R. Preparation and characterization of aligned porous PCL/zein scaffolds as drug delivery systems via improved unidirectional freeze-drying method. *Mater. Sci. Eng. C.*, 2016; **68**: 613–22.
25. Wong, B.S., Teoh, S.-H., Kang, L. Polycaprolactone scaffold as targeted drug delivery system and cell attachment scaffold for postsurgical care of limb salvage. *Drug Deliv. Transl. Res.*, 2012; **2**: 272–83.
26. Kumari, A., Yadav, S.K., Yadav, S.C. Biodegradable polymeric nanoparticles based drug delivery systems. *Colloids Surfaces B Biointerfaces.*, 2010; **75**: 1–18.
27. Wu, J.-B., Fong, Y.-C., Tsai, H.-Y., Chen, Y.-F., Tsuzuki, M., Tang, C.-H. Naringin-induced bone morphogenetic protein-2 expression via PI3K, Akt, c-Fos/c-Jun and AP-1 pathway in osteoblasts. *Eur. J. Pharmacol.*, 2008; **588**: 333–41.
28. Wang, L., Zhang, Y.-G., Wang, X.-M., Ma, L.-F., Zhang, Y.-M. Naringin protects human adipose-derived mesenchymal stem cells against hydrogen peroxide-induced inhibition of osteogenic differentiation. *Chem. Biol. Interact.*, 2015; **242**: 255–61.
29. Wong, R.W.K., Rabie, A.B.M. Effect of naringin on bone cells. *J. Orthop. Res.*, 2006; **24**: 2045–50.
30. Pang, W.-Y., Wang, X.-L., Mok, S.-K., Lai, W.-P., Chow, H.-K., Leung, P.-C., Yao, X.-S., Wong, M.-S. Naringin improves bone properties in ovariectomized mice and exerts oestrogen-like activities in rat osteoblast-like (UMR-106) cells. *Br. J. Pharmacol.*, 2010; **159**: 1693–703.
31. Caetano, G.F., Bártolo, P.J., Domingos, M., Oliveira, C.C., Leite, M.N., Frade, M.A.C. Osteogenic Differentiation of Adipose-derived Mesenchymal Stem Cells into Polycaprolactone (PCL) Scaffold. *Procedia Eng.*, 2015; **110**: 59–66.
32. Lin, F., Du, S., Liu, D., Hu, Q., Yu, G., Wu, C., Zheng, G., Xie, D., Li, X., Chang, B. Naringin promotes osteogenic differentiation of bone marrow stromal cells by up-regulating Foxc2 expression via the IHH signaling pathway. *Am. J. Transl. Res.*, 2016; **8**: 5098–107.
33. Ji, Y., Wang, L., Watts, D.C., Qiu, H., You, T., Deng, F., Wu, X. Controlled-release naringin nanoscaffold for osteoporotic bone healing. *Dent. Mater.*, 2014; **30**: 1263–73.